Tennessee Valley Authority
Office of Natural Resources
Division of Air and Water Resources
Water Systems Development Branch

A NUMERICAL SIMULATION OF HEAT TRANSFER IN EVAPORATIVE COOLING TOWERS

Report No. WR28-1-900-110

Prepared by
Dudley J. Benton

Norris, Tennessee
September 1983

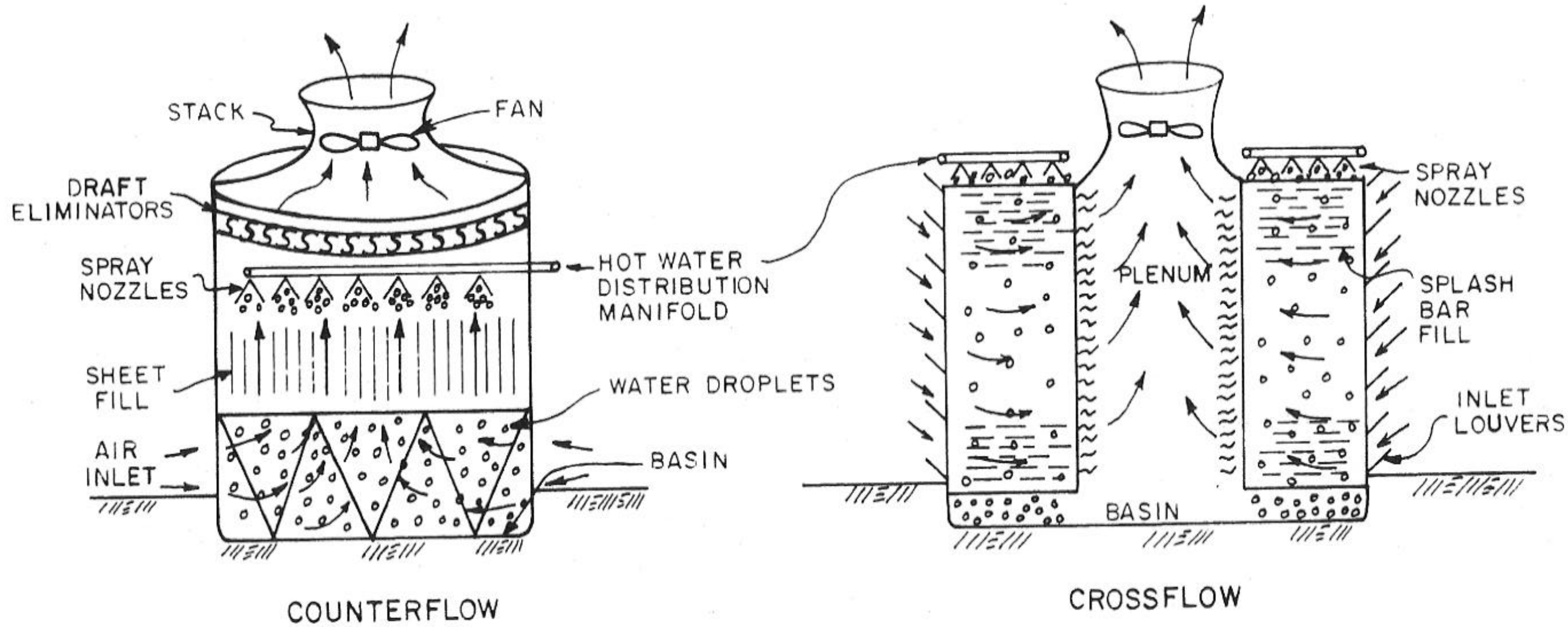

Figure 1: Schematic of Mechanical-Induced-Draft Cooling Towers

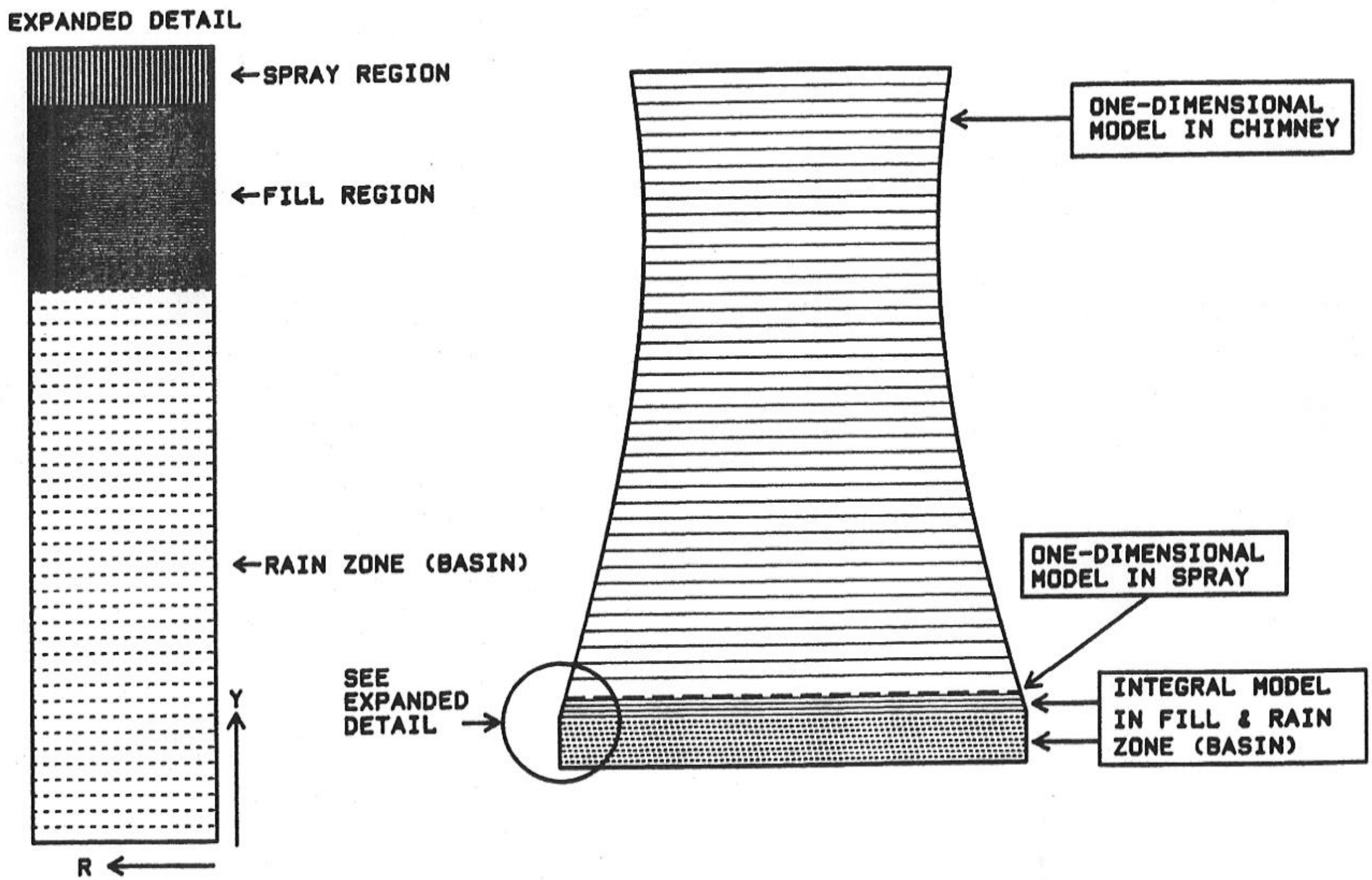

Figure 2. Actual Grid Spacing Used in Natural-Draft Counterflow Towers

MASS, LATENT-, AND SENSIBLE-HEAT TRANSFERS

The heat transfer within an evaporative cooling tower may be expressed in terms of sensible and evaporative (or latent) heat transfer. The differential sensible-heat transfer rate, dQ_s, from the water droplets in the cooling tower is expressed as the product of the local heat transfer coefficient, H; and the temperature difference between the local water temperature, T_w, and the local air dry-bulb temperature, T_{db}; and the differential interfacial area, dA_i:

$$dQ_s = H\ (T_w - T_{db})\ dA_i \qquad (1)$$

The differential evaporative mass transfer rate, dE, is similarly related to the driving potential, B, and the mass transfer coefficient K:

$$dE = K\ B\ dA_i \qquad (2)$$

where the mass transfer driving potential is defined in terms of the mass fraction, f, of the diffusing species (water) in the far field; and the mass fraction of the diffusing species at the interface, f_s, which is assumed to be the saturation value [2]. This relationship is defined by

$$B = \frac{f_s - f}{1 - f_s} \qquad (3)$$

In the case of mixtures of air and water vapor, it is more convenient to express the mass transfer driving potential in terms of the absolute humidity, ω, than the mass fraction, f. The relationship between absolute humidity and mass fraction is

$$f = \frac{\omega}{1+\omega} \qquad (4)$$

The differential evaporative mass transfer rate, dE, may then be expressed in terms of the absolute humidity by combining Equations 2, 3, and 4

$$dE = K \frac{(\omega_s - \omega)}{(1+\omega)} dA_i \qquad (5)$$

The differential mass transfer rate is related to the differential latent-heat transfer rate, dQ_e, through the enthalpy of saturated water vapor, h_g:

$$dQ_e = h_g \, dE \qquad (6)$$

The sum of the differential sensible- and latent-heat transfer rates is the differential total heat transfer rate, dQ_t:

$$dQ_t = dQ_s + dQ_e \qquad (7)$$

The differential total heat transfer rate is also related to the differential temperature change, dT_w, of the water, the constant-pressure specific heat of the water, C_{pw}, and the mass flowrate of the water, L, by the conservation-of-energy principle,

$$dQ_t = - \sout{L C_{pw} dT}_w \quad - d(L C_{pw} T_w)$$

The differential interfacial area, dA_i, within a differential volume, dx dy dz, of fill is expressed

$$dA_i = a \, dx \, dy \, dz \qquad (8)$$

where a is the interfacial area per unit volume.

The three transfer equations of interest are then

$$dQ_s = Ha \, (T_w - T_{db}) \, dx \, dy \, dz \qquad (9)$$

$$dE = Ka \frac{(\omega_s - \omega)}{(1 + \omega)} dx \, dy \, dz \qquad (10)$$

$$dQ_e = h_g \, Ka \frac{(\omega_s - \omega)}{(1 + \omega)} dx \, dy \, dz \qquad (11)$$

For cylindrical coordinates dx dy dz is replaced with $2 \pi r \, dr \, d\theta \, dy$.

CONSERVATION EQUATIONS

The simulation of the cooling tower transfer processes is based on the following conservation equations:

1. Conservation of mass of air
2. Conservation of mass of water vapor
3. Conservation of energy for the gas phase
4. Conservation of energy for the water phase.

These conservation equations in conjunction with the Bernoulli equation [3] (with headloss included) constitute the set of equations solved in the present simulation. The form of the Bernoulli equation used is

$$p_1 + \frac{\rho_1 V^2{}_1}{2g_c} + \frac{\rho_1 g y_1}{g_c} = p_2 + \frac{\rho_2 V^2{}_2}{2gc} + \frac{\rho_2 g y_2}{g_c} + \text{losses} \qquad (12)$$

where the subscripts 1 and 2 represent two locations along a streamline, p is the pressure, ρ is the density, V is the total velocity, g_c is Newton's constant, g is the acceleration of gravity, and y is the elevation. These equations are applied in their steady-state, steady-flow form. The independent variables are the horizontal distance, x, vertical distance, y, total mass flowrate of water, L, inlet water temperature, T_h, and the ambient wet- and dry-bulb temperatures (T_{wb} and T_{db}, respectively). The dependent variables in the conservation equations are the air velocity, V, the absolute humidity, ω, the enthalpy of the air-water vapor mixture, h_a, the water temperature, T_w, and pressure, p. The auxiliary quantitities, wet bulb temperature, dry-bulb temperature, and density are determined using the following thermodynamic relationships for air-water vapor mixtures from computed values of ω, h_a, and p:

$$h_a = \int_0^{T_{db}} C_{pa}\, dT + \omega\, h_g \qquad (13)$$

where C_{pa} is the constant-pressure specific heat of dry air;

$$\rho = \frac{P}{T_{db} + 459.67} \quad \frac{1+\omega}{R_a + \omega R_w} \tag{14}$$

where R_a and R_w are the ideal gas constants for dry air and water vapor, respectively;

$$h_a = \int_o^{T_{as}} C_{pa}\, dT + \omega_s\, h_g \tag{15}$$

where T_{as} is the adiabatic saturation temperature which is assumed to be equivalent to the wet-bulb temperature, T_{wb}; and ω_s is the absolute humidity of saturated air at T_{as}. These relationships are given in Reference 4. The property values are tabulated in References 5 and 6.

The interrelationship among the dependent and independent variables is evident from the formulation of the conservation equations that follow. The conservation of <u>mass for the water vapor</u> within a control volume is expressed

$$\iiint Ka \frac{(\omega_s - \omega)}{(1+\omega)}\, dx\, dy\, dz = \iint \frac{\omega\rho\ V \cdot dA}{1+\omega} \tag{16}$$

where $V \cdot dA$ is dot product of the two vectors V and dA. The conservation of <u>energy for the air</u> within a control volume is

$$\iiint [h_g\ Ka \frac{(\omega_s - \omega)}{(1+\omega)} + Ha\, (T_w - T_{db})]\, dx\, dy\, dz = \iint \frac{h_a \rho\ V \cdot dA}{1+\omega} \tag{17}$$

Finally, the conservation of <u>energy for the water</u> within a control volume is expressed

$$L\ C_{pw}\, \Delta T_w = -\iiint [h_g\ Ka \frac{(\omega_s - \omega)}{(1+\omega)} + Ha(T_w - T_{db})]\, dx\, dy\, dz \tag{18}$$

MODELING ASSUMPTIONS

1. Steady-state, steady-flow;
2. Two-dimensional symmetry (i.e., lateral symmetry in cartesian

coordinates and circumferential symmetry in cylindrical coordinates);

3. Wet-bulb temperature is equivalent to adiabatic saturation temperature;
4. The cooling tower is externally adiabatic (thus, in the case of a natural-draft tower, the enthalpy of the air is constant in the chimney);
5. The atmosphere around a natural-draft tower is assumed to be isentropic, thus the ambient pressure may be related to the elevation by the following equations [3]:

$$\frac{P_a}{P_{ao}} = (1 - \gamma\alpha)^{\gamma} \tag{19}$$

$$\alpha = \frac{gy\rho_{ao}}{g_c P_{ao}} \tag{20}$$

$$\gamma = \frac{C_{pa}-C_{va}}{C_{pa}} \tag{21}$$

6. The water flows vertically downward.
7. In round counterflow towers the air flows between colinear hyperboloid pathlines.

Modeling the Rain and Fill Zones in a Counterflow Tower

In the rain and fill zones of counterflow towers, the transport and conservation equations are solved using an integral technique [7]. The air in these zones is assumed to flow between colinear hyperboloid pathlines (see Figures 4 and 5). The fraction of the total airflow which flows between each of these pathlines is computed from the Bernoulli equation

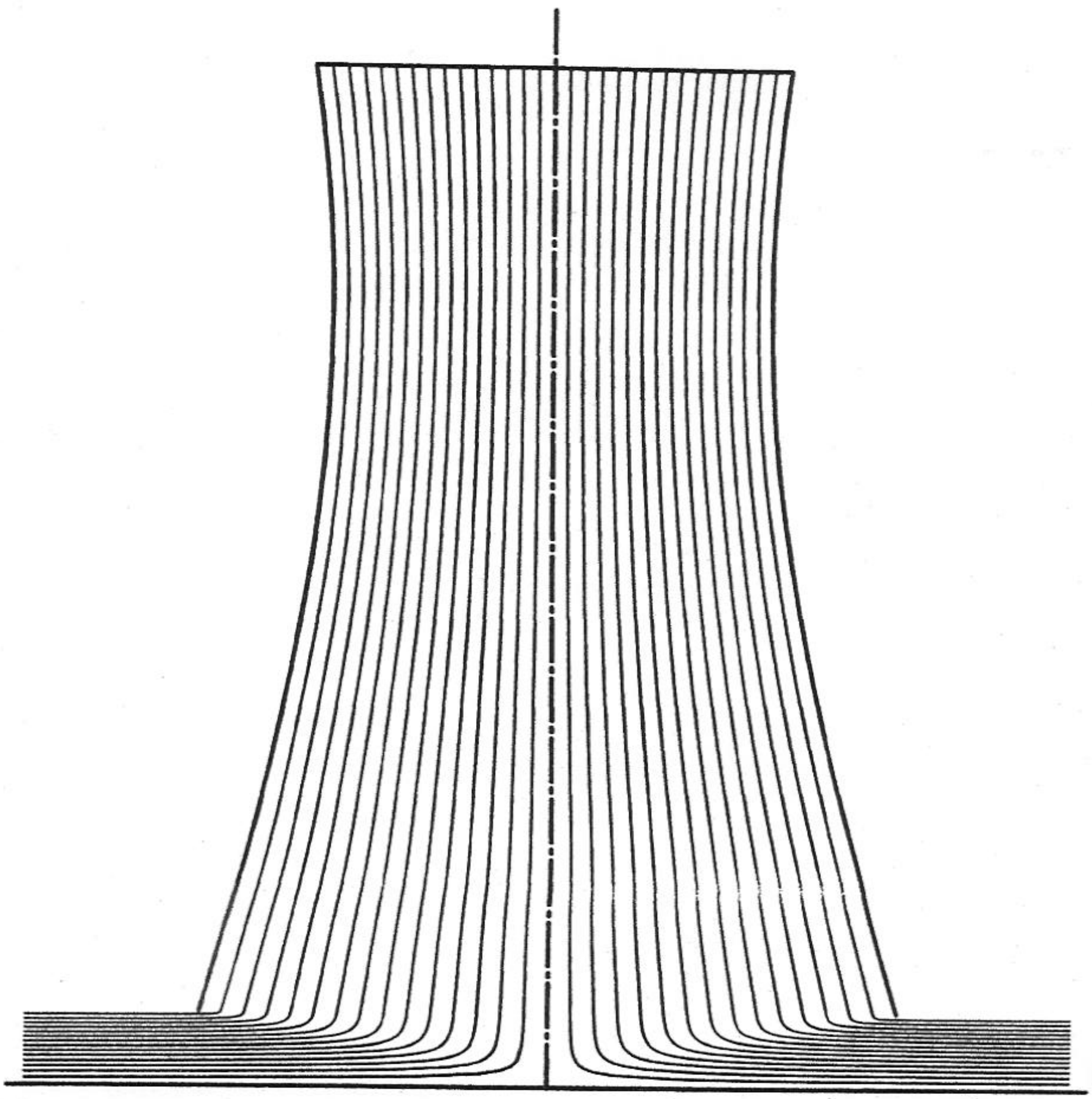

Figure 4. Location of Assumed Airflow Pathlines in a Natural-Draft Counterflow Tower

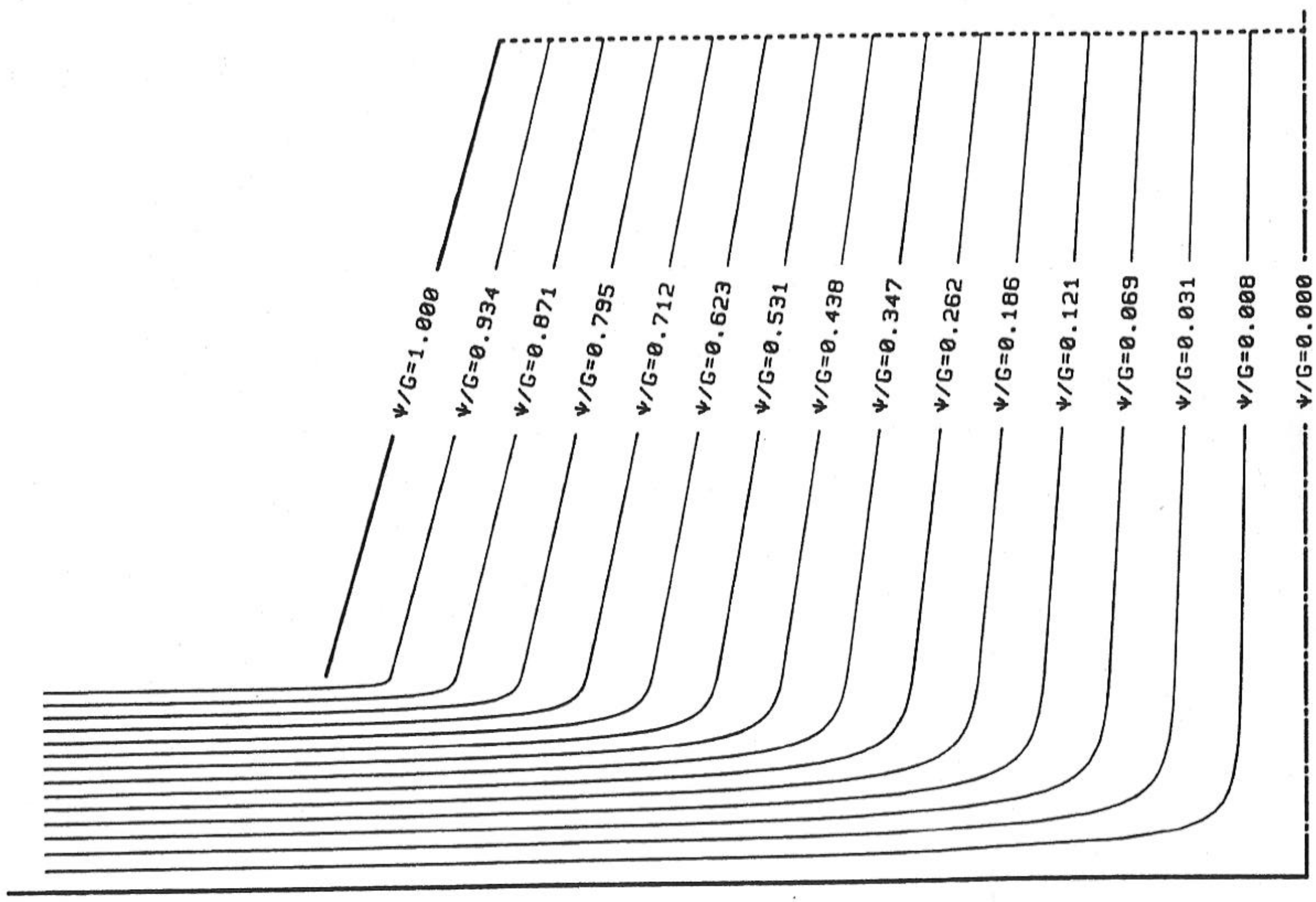

Figure 5. Expanded Detail of Assumed Airflow Pathlines in a Natural-Draft Counterflow Tower

(with headloss) and reflects the resistance to flow in the rain zone as well as the fill. The flow-resistance characteristics of the fill may vary radially (from path to path) as well as vertically. At each elevation the pressure-drop and transfer characteristics of the fill are numerically integrated in the radial direction to obtain average characteristics. In this radial integration, the pressure-drop, mass-, and heat-transfer characteristics are weighted (for each path within the fill) by the velocity head and airflow and waterflow, respectively. These average characteristics are then used to solve the one-dimensional integral governing equations.

Pressure Rise Across the Fan in Mechanical-Draft Towers

In mechanical-draft towers the pressure rise across the fan, Δp_{fan}, is computed using the following relationship:

$$\Delta p_{fan} = \frac{550\ \eta_{fan}\ W_{fan}\ \rho_{fan}}{G} \qquad (22)$$

where η_{fan} and W_{fan} are the efficiency and energy input to the fan, respectively, and ρ_{fan} is the density of the air immediately upstream of the fan. The fan efficiency is an implicit function of airflow, air density, input power, and the pressure drop across the fill. The functional relationship for fan efficiency must be determined from field or laboratory measurements and supplied to the computer program. The computer program uses a cubic iteration to solve the pressure balance at the fan for the airflow, G, and the fan efficiency, η_{fan}.

Fill Transfer Characteristics

Most currently available fill transfer characteristics (e.g., [1]) have been obtained through Merkel's analysis [8] which combines the sensible-heat and mass transfer. The algebraic manipulation employed by Merkel eliminates sensible-heat transfer from the equation leaving only the mass transfer. Merkel referred to the resulting transfer coefficient as the "total transfer coefficient;" however, according to Merkel's notation, it is equivalent to the mass transfer coefficient, Ka, used in the present analysis.

A sensible-heat transfer coefficient, Ha, as well as mass transfer coefficient, Ka, are required by the present analysis. In the event that only one is available, the Lewis analogy is applied [9]. In contrast to the Merkel analysis, which assumes a constant Lewis number, Le, of unity, the present model uses a local Lewis number that varies with temperature and absolute humidity and the constant-pressure specific heat, C_{pa}, to obtain separate sensible-heat and mass transfer coefficients and to extend the measured values of Ka and Ha to temperatures and absolute humidities other than those measured. The Lewis analogy is expressed by:

$$Ha = C_{pa}\ Le\ Ka \tag{23}$$

The local Lewis number is determined from the local molecular thermal conductivity, κ, density, ρ, diffusion coefficient, D, and constant-pressure specific heat:

$$Le = \frac{\kappa}{\rho\ DC_{pa}} \tag{24}$$

where κ, ρ, and C_{pa} depend on both temperature and absolute humidity and D depends only on temperature. No hot-water temperature correction factor is applied in the present model.

DISCRETIZATION OF COOLING TOWER

Simulation of the mass and heat transfer processes in the cooling tower requires that the tower be discretized, or divided into computational cells. Each cell is treated as a control volume, and the governing equations are applied to each. At each cell the computed conditions from adjacent upstream cells are utilized. These conditions (e.g., enthalpy, velocity, density, temperature, absolute humidity, and pressure) are defined at nodes located at the mid-points of the cell boundaries. The use of boundary nodes assures conservation of mass and energy from cell to cell (viz., the mass leaving the east face of one cell enters the west face of the adjacent cell by virtue of common storage of the variables, see Figure 6). Applying the Bernoulli, conservation, and transfer equations (i.e., 12, 16, 17, and 18) to each cell results in a set of nonlinear simultaneous equations (four for each cell) implicitly relating the four dependent variables (viz. ω, h_a, T_w, p). The auxiliary quantities (i.e., T_{wb}, T_{db}, ρ) are related to the dependent variables by the thermodynamic relationships (i.e., Equations 13, 14, and 15). These implicit nonlinear simultaneous equations are solved using the Gauss-Seidel method (viz. point-by-point successive substitution) [7]. This solution procedure is detailed subsequently.

Crossflow Towers

Figure 6 illustrates the cell and node configuration for crossflow towers. In this scheme the water temperature and the vertical air velocity are defined at the top and bottom of each cell (referred to as the north and south boundaries, respectively) while the enthalpy, humidity, and horizontal air velocity are defined at the left and right of each cell (referred to as the east and west boundaries, respectively).

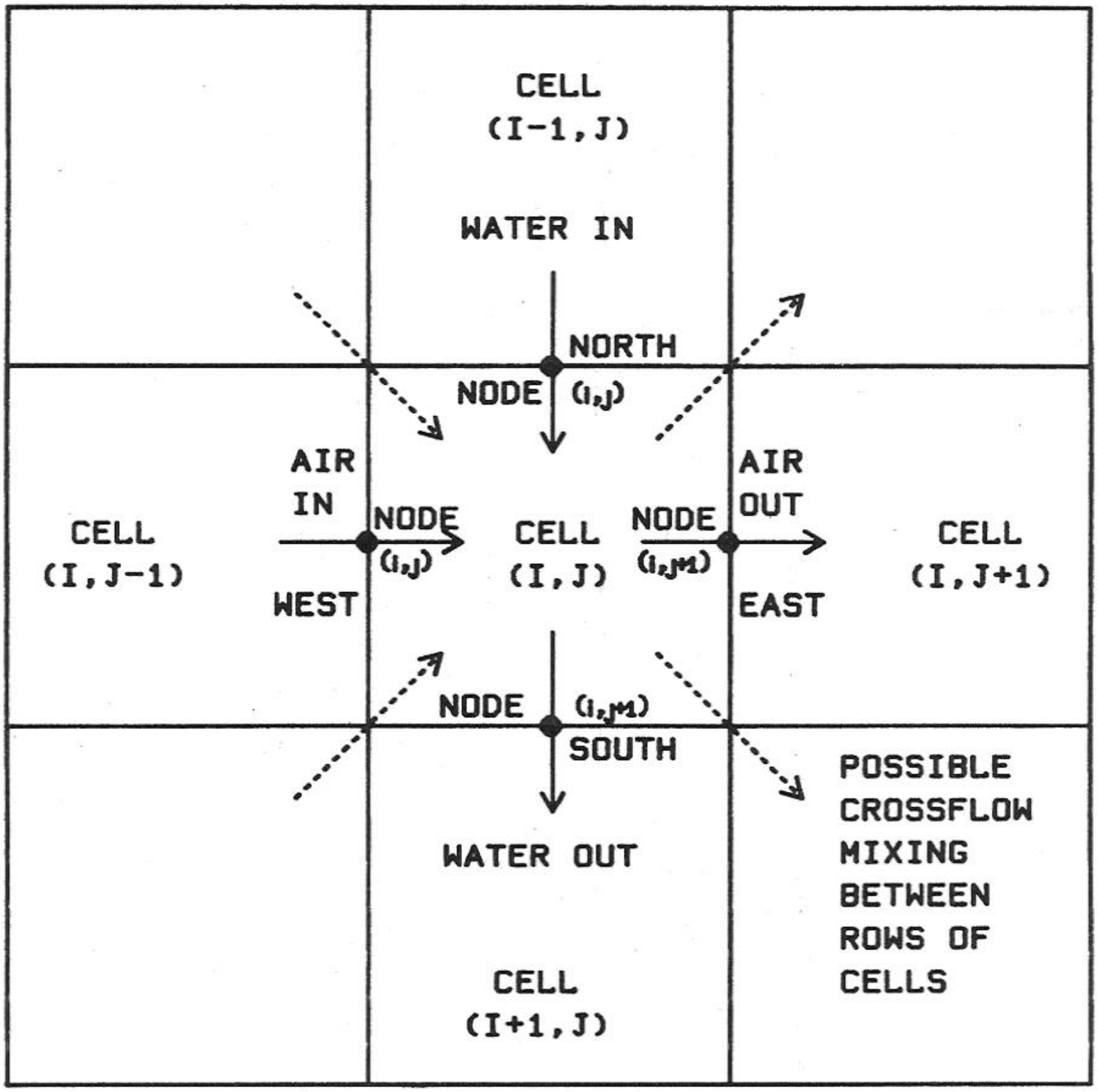

Figure 6. Node and Cell Index Notation Showing Air and Water Paths

The distribution of cells in the fill zone gives the solution a two-dimensional character (assuming circumferential or lateral symmetry). A one-dimensional distribution of cells is considered sufficient in the chimney region of natural-draft towers and the fan and recovery stack region of mechanical-draft towers.

The integrals in the conservation equations for the individual cells are evaluated using only the values of absolute humidity, dry-bulb temperature, saturated absolute humidity, and air enthalpy at the exit planes of each cell. For example, ω_s is computed based on the water temperature leaving the cell (viz. at the south face). This integration results in a pure implicit scheme which is more stable numerically than an explicit scheme using inlet quantities. The exclusive use of exit quantities precludes local violations of the second law of thermodynamics which result from overshoot when using inlet or average quantities. With the present implicit scheme, satisfying the second law of thermodynamics takes precedence over satisfying a transfer equation. Although the transfer equations may not always be satisfied with the present implicit scheme, the conservation equations are always satisfied.

Counterflow Towers

The arrangement of cells and nodes for counterflow towers is illustrated in Figure 2. The distribution of cells is such that the solution is one-dimensional. The integrals in the conservation equations for the individual cells are evaluated using only the values of absolute humidity, air dry-bulb temperature, saturated absolute humidity, and the air enthalpy at the exit planes of each cell.

The rain zone, fill, spray zone, and chimney (or fan and recovery stack) are separated, and heat transfer and pressure drop coefficients appropriate to the respective regions applied. Again, the temperature, velocity, density, pressure, enthalpy, and absolute humidity are specified at the midpoints of the cell boundaries.

BOUNDARY CONDITIONS

Crossflow Towers

The boundary condition for the water is specified at the top row of cells (top of the fill). The entering waterflow distribution can be arbitrarily specified. The boundary conditions for the air are inlet wet- and dry-bulb temperatures, pressure, and velocity, as well as the ambient pressure at the exit of the chimney. An arbitrary distribution of inlet wet-and dry-bulb temperatures can be specified. The ambient far-field velocity is assumed to be zero.

Counterflow Towers

The boundary condition for the water is specified at the point of discharge from the spray nozzles. The entering waterflow distribution can be arbitrarily specified. The boundary conditions for the air are inlet wet- and dry-bulb temperatures, pressure, and velocity as well as the ambient pressure at the exit of the chimney. An arbitrary distribution of inlet wet- and dry-bulb temperatures can be specified.

SOLUTION PROCEDURE

Crossflow Towers

The iterative solution process illustrated in the flowchart, Figure 7, is initiated by solving a simplified point model to obtain initial values for the air flowrate and wet- and dry-bulb temperature at the exit of the cooling tower. The results are used to provide an initial distribution of the absolute humidity, enthalpy, and wet- and dry-bulb temperatures throughout the tower. Linear interpolation from entrance to exit is used to obtain initial values at intermediate locations.

The computation of sensible- and latent-heat transfer rates starts in the upper lefthand corner cell and proceeds one column at a time. The computation for each cell is an iterative process since the driving potential for the transfers utilizes the conditions at the exit. After the energy transfer in the cells located in the fill has been computed, the air is assumed to be thoroughly mixed as it flows through the chimney (or fan) without further heat or mass transfer (i.e., the two-dimensional analysis within the fill region is patched onto a one-dimensional analysis at the exit of the fill).

With the temperatures and absolute humidities established and a trial airflow estimated, an evaluation of the airflow distribution is undertaken. The Bernoulli equation (with headloss) and the conservation of mass (of air) is applied to each cell. The airflow distribution is solved in the same manner as a branched pipe network having interconnecting paths which permit crossflow.

A solution of the Bernoulli and conservation of mass of air equations provides values of velocity and pressure at the exit face of each

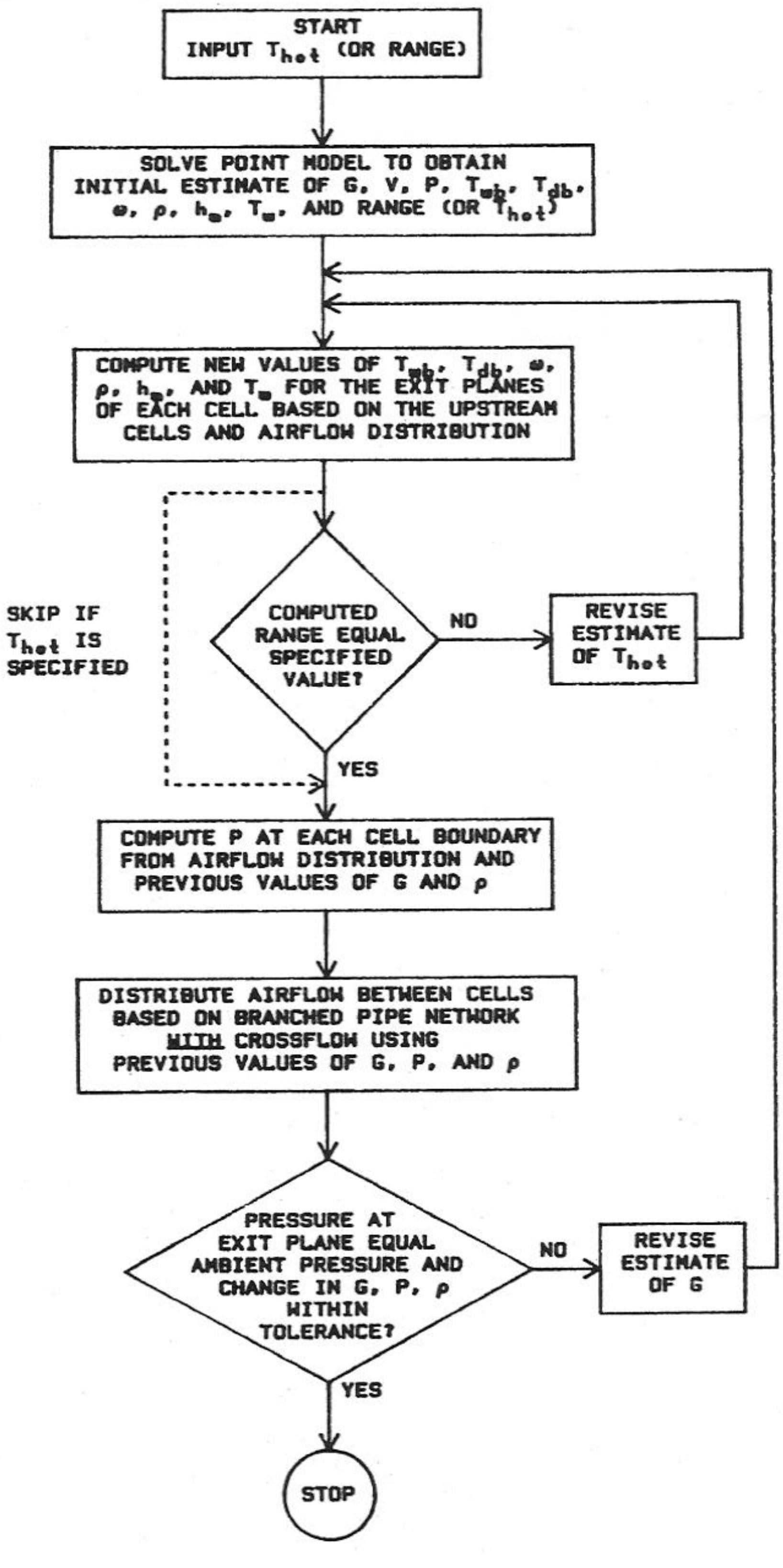

Figure 7. Flowchart of Solution Procedure for Crossflow Towers

cell within the fill. An average velocity is computed for the plenum and the Bernoulli equation used through the chimney or fan. The fan and recovery stack in mechanical-draft towers are each modeled as a single cell. In natural-draft towers the chimney is discretized into a number of cells (see Figure 3).

Based on the new flow distribution, revised values of temperature, enthalpy, and humidity ratio are computed. These values reflect vertical mixing between adjacent cells in the fill. The sensible- and latent-heat trasfer rates in the various cells are recomputed using the temperatures, densities, and velocities from the preceding step.

The iterative process is considered to have converged when the computed pressure at the exit plane corresponds to the ambient pressure.

Counterflow Towers

The iterative solution process illustrated in the flowchart, Figure 8, is initiated by solving a simplified point model to obtain initial values for the air flowrate and wet- and dry-bulb temperature at the exit of the cooling tower. The results are used to provide an initial distribution of the absolute humidity, enthalpy, and wet- and dry-bulb temperatures throughout the tower. Linear interpolation from entrance to exit is used to obtain initial values at intermediate locations. An initial estimate of the airflow distribution is computed based on the potential flow solution for a cylindrical jet impinging on an infinite wall perpendicular to its centerline.

The solution procedure is initiated in the rain zone and is based on an assumed cold-water temperature so that heat transfer computations can proceed. When the computations are advanced to the spray nozzles a check is made to determine if the computed hot water temperature corres-

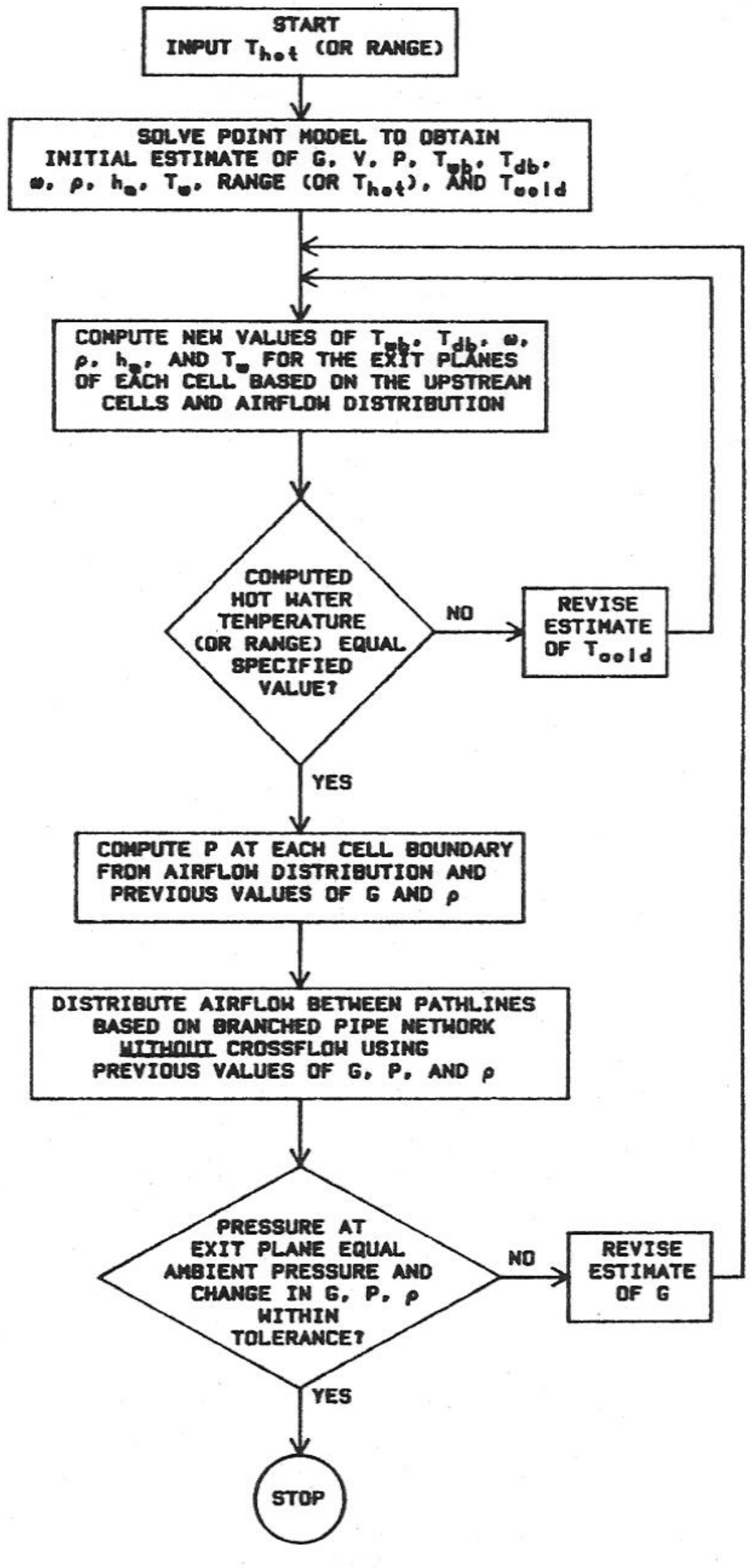

Figure 8. Flowchart of Solution Procedure for Counterflow Towers

ponds to the specified hot water temperature. If the computed and specified hot water temperatures do not agree, the cold water temperature is adjusted and the heat transfer computations redone. When the computed and specified hot water temperatures agree, the pressure computations are performed. The airflow within the rain and fill zones is redistributed among the pathlines (see Figures 4 and 5) according to the the Bernoulli equation (with headloss included) such that dynamic pressure (i.e., $p+\rho v^2/2g_c$) at the top of the fill is uniform in the radial direction. The computed pressure at the exit plane is then compared to the specified ambient pressure. If the pressures are not in agreement, the airflow is appropriately adjusted and the heat transfer computations restarted. This series of computations continues until the computed hot water temperature and exit pressure correspond with the values prescribed as boundary conditions.

FEATURES OF THE MODEL

The present model has been developed into a computer program, coded in FORTRAN 77, comprised of a main program and 38 subprograms in approximately 7000 statements. The computer program requires 109K bytes (1 byte = 8 binary bits) of memory. However, only 33K bytes are required for any one geometry (i.e., mechanical-crossflow) which permits the use of the program on many microprocessors. The execution time is approximately 30 seconds on an HP-1000F minicomputer or 1 second on an IBM-370.

The computer program models mechanical induced-draft crossflow, mechanical induced-draft counterflow (round-type), natural-draft crossflow, and natural-draft counterflow towers.

Either the hot water temperature or the range may be specified, and the water distribution may be uniform or nonuniform. The ambient wet- and dry-bulb temperatures may be uniform or an arbitrary vertical profile may be specified.

The fan efficiency in mechanical-draft towers may be specified as a constant or as a function of flow, pressure differential, power input, etc.

Any number of fill types may be specified at symmetric locations within the fill region. Thus the computer program can handle hybrid fills as well as voids and obstructions. This feature is illustrated in Figure 9.

The computer program also provides dimensionless graphs of velocity, pressure, temperature, etc., and a map of fill type and location.

Numerical Formulation of the Conservation Equations

The finite-integral formulation of the conservation equations (viz. Reynolds Transport [3]) is used rather than the finite-difference formulation [7]. The two formulations are equivalent mathematically. However, in finite-precision arithmetic as performed by a computer they are not. There is a distinct advantage to the finite-integral formulation over the finite-difference: the numerical evaluation of integrals involves the addition of many numbers of the same order of magnitude, whereas the numerical evaluation of differences involves the subtraction of many numbers of same order of magnitude. Subtraction of numbers of the same order of magnitude requires greater precision to obtain the same accuracy in the result than does addition. As the number of cells increases the difference between quantities in any two adjacent cells decreases, thus requiring even greater precision with a finite-difference formulation. This problem is not encountered with the finite-integral formulation. Thus the choice of the

```
                 SPLASH BAR FILL ONLY
-----------------                    -----------------
\GGGGGGGGGGGGGGGG^                   \                ^
\GSSSSSSSSSSSSSSS^                   \ 1 33  5  77   9^
\GSSSSSSSSSSSSSSS^                   \ 1 33  5  77   9^
\GSSSSSSSSSSSSSSS^                   \ 1 33  5  77   9^
\GSSSSSSSSSSSSSSS^                   \ 1 33  5  77  99^
\GSSSSSSSSSSSSSSS^                   \ 1 33  5  77  99^
\GSSSSSSSSSSSSSSS^                   \ 1 33  5  77  99^
\GSSSSSSSSSSSSSSS^                   \ 1  3  5  77  99^
\GSSSSSSSSSSSSSSS^    AIR FLOW ->    \ 1  3  5  77  99^
\GSSSSSSSSSSSSSSS^                   \ 1  3  55 77  99^
\GSSSSSSSSSSSSSSS^                   \ 1  3  55 77  99^
\GSSSSSSSSSSSSSSS^                   \ 1  3  55 77  99^
\GSSSSSSSSSSSSSSS^                   \ 1  3  55 77  99^
\GSSSSSSSSSSSSSSS^                   \ 1  3  55 77  99^
\GSSSSSSSSSSSSSSS^                   \ 1  3  55  7  99^
\GSSSSSSSSSSSSSSS^                   \ 1  3  55  7   9^
-----------------                    -----------------
 FILL ARRANGEMENT                     VELOCITY DISTRIBUTION
  G=GHOST NODE                       1=6.35 FPS    9=7.30 FPS
  S=SPLASH BAR FILL
  \=INLET LOUVER
  ^=DRIFT ELIMINATOR


SPLASH BAR FILL WITH HIGH RESISTANCE FILL IN CENTER
-----------------                    -----------------
\GGGGGGGGGGGGGGGG^                   \                ^
\GSSSSSSSSSSSSSSS^                   \      7 99 77777^
\GSSSSSSSSSSSSSSS^                   \      7 99 77777^
\GSSSSSSSSSSSSSSS^                   \      7 99 77777^
\GSSSSSSSSSSSSSSS^                   \      7 99 77777^
\GSSSSSSSSSSSSSSS^                   \      7 99 77777^
\GSSSSSSSRSSSSSSS^                   \      7 3 777777^
\GSSSSSSRRRSSSSSS^                   \      7  15 7777^
\GSSSSSRRRRRSSSSS^    AIR FLOW ->    \       1 115 777^
\GSSSSSSRRRSSSSSS^                   \      7  15 7777^
\GSSSSSSSRSSSSSSS^                   \      7 3 777777^
\GSSSSSSSSSSSSSSS^                   \      7 99 77777^
\GSSSSSSSSSSSSSSS^                   \      7 99 77777^
\GSSSSSSSSSSSSSSS^                   \      7 99 77777^
\GSSSSSSSSSSSSSSS^                   \      7 99 77777^
\GSSSSSSSSSSSSSSS^                   \      7 99 77777^
-----------------                    -----------------
 FILL ARRANGEMENT                     VELOCITY DISTRIBUTION
  R=HIGH RESISTANCE FILL             1=3.30 FPS    9=7.10 FPS


        SPLASH BAR FILL WITH DIAGONAL FILM FILL
-----------------                    -----------------
\GGGGGGGGGGGGGGGG^                   \                ^
\GFFSSSSSSSSSSSSS^                   \  577   3   9999^
\GSSFFSSSSSSSSSSS^                   \  5 7   3   9999^
\GSSSSFFSSSSSSSSS^                   \  1577  93   999^
\GSSSSSSFFSSSSSSS^                   \  1577  93   999^
\GSSSSSSSSFFSSSSS^                   \  7 577 993   99^
\GSSSSSSSSSSFFSSS^                   \  7 577 993   99^
\GSSSSSSSSSSSFFSS^                   \  77 57 9993  99^
\GFFSSSSSSSSSSSFF^    AIR FLOW ->    \  77 57 9993  99^
\GSSFFSSSSSSSSSSS^                   \  777  7   93  9^
\GSSSSFFSSSSSSSSS^                   \  777  7   93  9^
\GSSSSSSFFSSSSSSS^                   \  777      993  ^
\GSSSSSSSSFFSSSSS^                   \  777      993  ^
\GSSSSSSSSSSFFSSS^                   \  777   7   993 ^
\GSSSSSSSSSSSSFFS^                   \  777   1 7  931^
\GSSSSSSSSSSSSSFF^                   \  777   3 7 9993^
-----------------                    -----------------
 FILL ARRANGEMENT                     VELOCITY DISTRIBUTION
  F=FILM FILL                        1=3.85 FPS    9=7.42 FPS
```

Figure 9. Air Velocity Distribution in a Crossflow Tower With Hybrid Fill

finite-integral formulation permits the present model to use single-precision (32 binary bit) numerical arithmetic rather than double-precision, effectively reducing the computational time by a factor of two.

COMPARISON WITH FIELD DATA AND CONCLUSIONS

The present model has been verified using cooling tower test data for mechanical-draft crossflow, natural-draft crossflow, and natural-draft counterflow towers. This verification includes uniform as well as hybrid fills. The tower locations and types used in the verification are listed in Table 1. Also listed in Table 1 are the ambient conditions, water loading, hot water temperature, and cold water temperature for each test case. Figure 10 provides a comparison of the test data and model predictions for the cold water temperature. The fill characteristics used in the model for this comparison with test data were taken from Lowe and Christie [1] without calibration or adjustment.

The present model is coded in FORTRAN77 and requires 109K bytes of memory. However, only 33K bytes of memory are required for any one particular geometry, which permits the use of the model on many microprocessors. The execution time on an HP-1000F minicomputer is approximately 30 seconds, making the present model relatively inexpensive to use.

The present model can be used to predict tower performance, reduce test data, and evaluate the effect on tower performance of modifications to existing towers. It can also be used to predict the performance of cooling towers which are being considered for construction, provided sufficient information is known, such as fill characteristics.

TABLE 1

Comparison of the Present Model and Field Data
For Cold Water Temperature

Location	Type	T_{hot}	T_{db}	T_{wb}	T_{cold} Field	T_{cold} Computed	Error
PSP	NDC	91.3	60.2	59.7	75.6	76.4	0.8
PSP	NDC	109.5	85.0	69.9	89.0	88.4	-0.6
PSP	NDC	104.8	68.6	66.9	84.4	83.9	-0.5
PSP	NDC	107.1	77.8	70.3	87.1	87.0	-0.1
PSP	NDC	111.1	85.8	68.9	85.8	85.7	-0.1
PSP	NDC	111.9	87.3	69.8	86.4	86.3	-0.1
PSP	NDC	110.1	53.1	47.3	81.3	82.5	1.2
PSP	NDC	92.3	39.0	35.8	74.5	73.0	-1.5
SNP	NDX	104.7	89.9	74.9	93.0	93.3	0.3
SNP	NDX	106.3	83.7	74.8	93.1	91.7	-1.4
SNP	NDX	99.9	56.5	47.9	77.6	77.7	0.1
SNP	NDX	100.5	53.4	49.5	77.5	77.9	0.4
BFNP	MDX	86.0	NA	55.1	73.2	73.6	0.4
BFNP	MDX	86.4	NA	57.5	74.1	74.5	0.5
BFNP	MDX	90.8	NA	55.6	75.6	76.1	0.5
BFNP	MDX	92.4	NA	50.3	74.7	75.3	0.6
BFNP	MDX	94.5	NA	56.8	77.7	78.2	0.5
BFNP	MDX	92.8	NA	60.3	78.2	78.5	0.3
BFNP	MDX	94.1	NA	61.5	79.3	79.4	0.1
BFNP	MDX	93.4	NA	48.2	75.3	75.6	0.3
BFNP	MDX	89.0	NA	48.7	72.8	73.4	0.6
BFNP Phelps	MDX	92.7	NA	61.4	78.5	79.1	0.6
BFNP Phelps	MDX	102.1	NA	59.6	81.4	81.7	0.3
BFNP Phelps	MDX	101.6	NA	61.8	82.4	83.0	0.6
BFNP Phelps	MDX	102.4	NA	64.1	83.4	84.0	0.6

LEGEND
MDX: Mechanical-draft crossflow
NDX: Natural-draft crossflow
NDC: Natural-draft counterflow
Phelps: With Phelps Fix

PSP: Paradise Steam Plant (TVA)
SNP: Sequoyah Nuclear Plant (TVA)
BFNP: Browns Ferry Nuclear Plant (TVA)

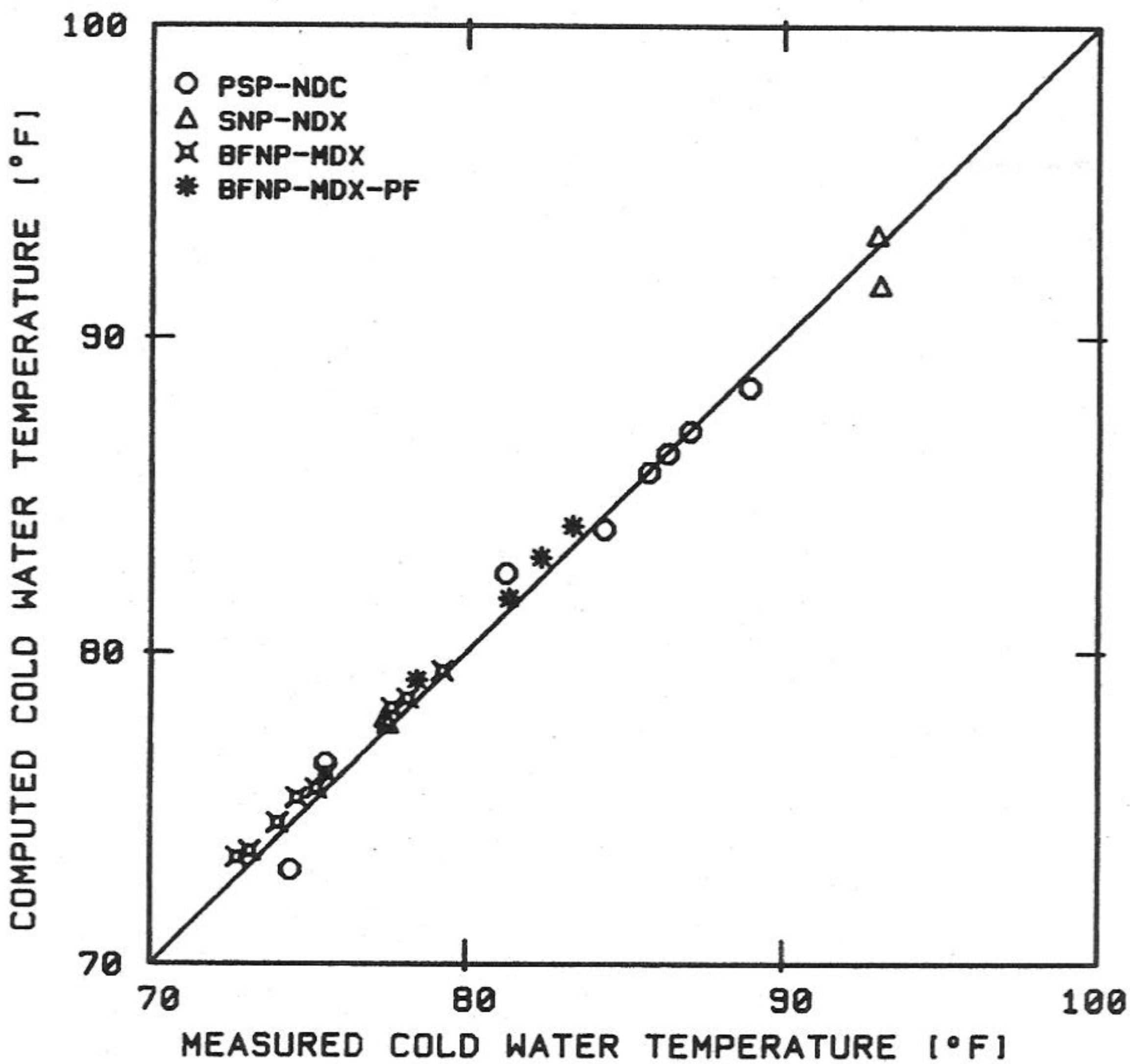

Figure 10. Comparison of Measured and Computed Cold Water Temperature

In conclusion the present model is an accurate, efficient, and inexpensive tool for analyzing the performance of existing towers or predicting the performance of alternate tower designs.

NOMENCLATURE

a	interfacial area per unit volume $[L^2/L^3]$
A	vector area (outward normal) $[L^2]$
A_i	interfacial area $[L^2]$
B	mass transfer driving potential
C_{pa}	constant-pressure specific heat of air $[E/mT]$
C_{va}	constant-volume specific heat of air $[E/mT]$
C_{pw}	constant-pressure specific heat of water $[E/mT]$
D	air/water vapor diffusion coefficient $[L^2/t]$
E	evaporation $[m/t]$
f	mass fraction of water in an air-water vapor mixture
f_s	mass fraction of water vapor at saturation
G	mass flowrate of dry air $[m/t]$
G''	mass flux of air $[m/L^2t]$
g	gravitational acceleration $[L/t^2]$
g_c	Newton's constant $[mL/Ft^2]$
H	heat transfer coefficient $[E/L^2tT]$
h_a	enthalpy of moist air (based on the mass of dry air) $[E/m]$
h_g	enthalpy of saturated water vapor $[E/m]$
i	vertical (y) index for nodes
I	vertical (y) index for cells
j	horizontal (x) or radial (r) index for nodes
J	horizontal (x) on radial (r) index for cells
K	mass transfer coefficient $[m/L^2t]$
L	mass flowrate of water $[m/t]$

Le	Lewis number
M	number of horizontal (x) or radial (r) cells
N	number of vertical (y) cells
p	pressure [F/L^2]
p_a	ambient pressure [F/L^2]
p_{ao}	ambient pressure at y=0 [F/L^2]
p_{sat}	saturation pressure of water [F/L^2]
Q_e	evaporative heat transfer [E/t]
Q_s	sensible-heat transfer [E/t]
Q_t	total heat transfer [E/t]
r	radial coordinate (outward from centerline) [L]
R_a	ideal gas constant for dry air [FL/m/T]
R_w	ideal gas constant for water vapor [FL/m/T]
T_{as}	adiabatic saturation temperatur [T]
T_{db}	dry-bulb temperature [T]
T_h	hot-water temperature [T]
T_w	water temperature (local) [T]
T_{wb}	wet-bulb temperature [T]
u	velocity in either the horizontal (x) or radial (-r) direction [L/t]
v	velocity in the vertical (y) direction [L/t]
V	velocity vector [L/t]
W_{fan}	work rate (power) of fan [E/t]
x	horizontal coordinate (from exterior to interior) [L]
y	vertical coordinate (from bottom upward) [L]
z	lateral coordinate

Greek

α	dimensionless elevation
γ	isentropic exponent
Δy	vertical dimension of a cell [L]
η	efficiency
θ	circumferential angle
κ	thermal conductivity of moist air [E/L/t/T]
λ	dimensionless pressure drop (in velocity heads)
ρ	density [m/L^3]
ρ_a	ambient air density [m/L^3]
ρ_{ao}	ambient air density at y=o [m/L^3]
Ψ	path function [m/t]
ω	absolute humidity (mass of water vapor/mass of dry air)
ω_s	absolute humidity at saturation

Units

[m]	= mass
[t]	= time
[L]	= length
[F]	= force
[E]	= energy
[T]	= temperature

REFERENCES

1. Lowe, H. J., and D. G. Christie, "Heat Transfer and Pressure Drop on Cooling Tower Packings and Model Studies of the Resistance of Natural-Draft Towers to Airflow," International Division of Heat Transfer, Part V, pp 933-950, American Society of Mechanical Engineers, New York.

2. Kays, W. M., Convective Heat and Mass Transfer, McGraw-Hill, 1966.

3. Streeter, Victor L., and E. B. Wylie, Fluid Mechanics 6th Ed., McGraw-Hill, New York, 1975.

4. Van Wylen, Gordon J., and Richard E. Sonntag, Fundamentals of Classical Thermodynamics 2nd Ed., Wiley, New York, 1973.

5. ASHRAE Handbook: Fundamentals, American Society of Heating, Refrigerating, and Air-Conditioning Engineers, New York, 1977.

6. Keenan, Joseph H., Frederick G. Keyes, Philip G. Hill, and Joan G. Moore, Steam Tables, Wiley, New York, 1969.

7. Ames, W. F., Nonlinear Partial Differential Equations in Engineering, Academic Press, New York, 1965.

8. Merkel, F., "Evaporative Cooling," Zeits. Verein deutscher Ingenieure, Vol. 70, pp 123-128, 1926.

9. Lewis, W. K., Transactions of the American Society of Mechanical Engineers, Vol. 44, p 329, 1922.